



Theoretical band energetics of Ba (M 0.5 Sn 0.5) O 3 for solar photoactive applications

Pramod H. Borse, Jae S. Lee, and Hyun G. Kim

Citation: [Journal of Applied Physics](#) **100**, 124915 (2006); doi: 10.1063/1.2401040

View online: <http://dx.doi.org/10.1063/1.2401040>

View Table of Contents: <http://scitation.aip.org/content/aip/journal/jap/100/12?ver=pdfcov>

Published by the [AIP Publishing](#)

Articles you may be interested in

[Artificial layered perovskite oxides A\(B0.5B'0.5\)O3 as potential solar energy conversion materials](#)

J. Appl. Phys. **117**, 055106 (2015); 10.1063/1.4907577

[\(Sr,Ba\)\(Si,Ge\)2 for thin-film solar-cell applications: First-principles study](#)

J. Appl. Phys. **115**, 203718 (2014); 10.1063/1.4880662

[Cationic \(V, Y\)-codoped TiO2 with enhanced visible light induced photocatalytic activity: A combined experimental and theoretical study](#)

J. Appl. Phys. **114**, 183514 (2013); 10.1063/1.4831658

[Band-engineered SrTiO3 nanowires for visible light photocatalysis](#)

J. Appl. Phys. **112**, 104322 (2012); 10.1063/1.4767229

[Investigation of the energy band structure of orthorhombic BaSi 2 by optical and electrical measurements and theoretical calculations](#)

Appl. Phys. Lett. **81**, 1032 (2002); 10.1063/1.1498865

Did your publisher get
18 MILLION DOWNLOADS in 2014?
AIP Publishing did.



THERE'S POWER IN NUMBERS. Reach the world with AIP Publishing.



Theoretical band energetics of $\text{Ba}(M_{0.5}\text{Sn}_{0.5})\text{O}_3$ for solar photoactive applications

Pramod H. Borse and Jae S. Lee^{a)}

Eco-friendly Catalysis and Energy Laboratory (NRL), Department of Chemical Engineering, Pohang University of Science and Technology, Pohang 790-784, South Korea

Hyun G. Kim

Busan Center, Korea Basic Science Institute, Busan 609-735, South Korea

(Received 1 August 2006; accepted 30 September 2006; published online 28 December 2006)

We report here a comparative study of the theoretically calculated electronic structures of cubic BaSnO_3 and cubic $\text{Ba}(M_{0.5}\text{Sn}_{0.5})\text{O}_3$ with $M=\text{Ti, V, Cr, Zr, Ce, and Pb}$, the tetravalent metal ions, to explore their possible efficacy for the visible light photocatalysis and solar energy conversion. We performed the calculations within the framework of density functional theory by using WIEN97 code. The $3d$ orbitals of Ti, V, and Cr, $4d$ of Zr, and the $4f$ and $6s$ orbitals of Ce and Pb, respectively, contributed to the bottom of the conduction band for narrowing of the band gap of cubic BaSnO_3 . Calculation of the frequency dependent absorption coefficient $I(\omega)$ of $\text{Ba}(M_{0.5}\text{Sn}_{0.5})\text{O}_3$ indicated that among the transition metal (Ti, V, Cr, and Zr) doped systems, Cr has comparatively higher visible absorption efficiency, whereas among other metal (Pb and Ce) systems, Pb showed significant absorption coefficient in low energy range ($E \leq 2$ eV). The comparison of the computed optical absorption coefficients shows that the $\text{Ba}(M_{0.5}\text{Sn}_{0.5})\text{O}_3$ systems can be arranged with respect to M as (i) $\text{Cr} > \text{V} > \text{Ti}$ among first row transition metals and (ii) $\text{Pb} > \text{Ce} > \text{Zr}$ among rest of tetravalent metals, in decreasing order of photoresponse towards low energy photons ($E \leq 2.5$ eV). © 2006 American Institute of Physics. [DOI: 10.1063/1.2401040]

I. INTRODUCTION

Recently photoactive perovskite metal oxides are gaining a lot of attention due to their ever-growing importance in solar energy conversion applications. Especially, the p -block systems with d^{10} perovskites have been recently shown^{1,2} to be effective in the visible light photocatalysis for H_2 generation, possibly due to their enhanced electron mobility in conduction band.² Though various perovskites under this d^{10} category have been explored and studied, still a lot remains unexplored. For example, BaSnO_3 (BSO) stannous system with d^{10} (Sn^{4+}) possesses a band gap energy (~ 3.4 eV) similar to best known photocatalysts,³⁻⁵ viz., TiO_2 , SrTiO_3 , ZnO , and ZnS , yet it has not been explored. Here we attempt the theoretical investigation on $\text{Ba}(M_{0.5}\text{Sn}_{0.5})\text{O}_3$ with $M=\text{Ti, V, Cr, Zr, Ce, and Pb}$ and evaluate its feasibility as a photoactive material.

The BaSnO_3 , a cubic perovskite structure (space group $Pm\bar{3}m$) and a unique n -type semiconducting metal oxide with a band gap of 3.4 eV,^{6,7} has been reported for its potential in optical,⁸ dielectric,^{9,10} and gas sensor applications. It has been sought recently to be an effective matrix for doping to achieve improved electrical properties.¹¹ Doped perovskites,¹²⁻¹⁸ by virtue of band gap tuning and consequent redshift in optical absorption of the UV-active original host matrix, have been shown to possess potential applications in visible light photocatalysis and solar energy conversion. Such doping is therefore very interesting in view of the

need of efficient photoactive materials for solar energy conversion applications. Thus, there is obvious need for exploration of optical applications of BSO and related systems. We present here the theoretical electronic structure calculation of $\text{Ba}(M_{0.5}\text{Sn}_{0.5})\text{O}_3$ with some tetravalent metal ions, viz., $M=\text{Ti, V, Cr, Zr, Ce, and Pb}$. Until now, there has been no report on the electronic properties of such systems. The present study focuses on the electronic structure of the cubic phase $\text{Ba}(M_{0.5}\text{Sn}_{0.5})\text{O}_3$. Further we made an attempt to correlate the obtained results to comment on the efficacy of the system for visible light photocatalytic application. We believe that the knowledge of electronic structure is desired and is very useful for understanding the optical candidacy of such systems for relevant applications, such as visible light photocatalysis.

II. METHODS AND COMPUTATIONAL DETAILS

Theoretical calculations were performed with the full potential linearized augmented plane-wave (FP-LAPW) method as implemented in the WIEN97 code with density functional theory (DFT) in generalized gradient approximation (GGA).¹⁸ In the LAPW method the unit cell is divided in two types of regions, the atomic spheres centered upon nuclear sites and the interstitial region between nonoverlapping spheres. Inside the atomic spheres, the wave functions are replaced by linear combination of atomlike wave functions, while in the intersphere region the wave functions are replaced by plane-wave-like expansion. The muffin-tin radii for Ba/ M , Sn, and O were chosen to be 2.0, 1.8, and 1.6 a.u., respectively, in these calculations. The convergence param-

^{a)}Author to whom correspondence should be addressed; electronic mail: jlee@postech.ac.kr

eter RK_{\max} was set to 6.0. The calculation was iterated with the charge convergence criteria of 0.0001. Self-consistency was carried out on a 10 or 18 k -point mesh in the irreducible Brillouin zone for BSO or $\text{Ba}(M_{0.5}\text{Sn}_{0.5})\text{O}_3$, respectively. In addition, a fine mesh of 100 k points in the irreducible Brillouin zone (BZ) of cubic unit cell was used to calculate the frequency dependent absorption coefficient $I(\omega)$ from real and imaginary parts of dielectric function $\epsilon(\omega) = \epsilon_1(\omega) + i\epsilon_2(\omega)$. A procedure similar to Gupta *et al.*¹⁹ and Borse *et al.*²⁰ was adopted for these calculations of $I(\omega)$ which is given as $I(\omega) = \sqrt{2}(\omega) [\sqrt{\epsilon_1(\omega)^2 + \epsilon_2(\omega)^2} - \epsilon_1(\omega)]^{1/2}$. The atomic coordinates were adopted from the literature.²¹ For the band structure calculations of cubic $\text{Ba}(M_{0.5}\text{Sn}_{0.5})\text{O}_3$ structure, a supercell with two BSO units was constructed from the available crystallographic data.²¹ The BaSnO_3 has the ideal cubic perovskite structure with the space group of $Pm\bar{3}m$, (Space Group No. 221) and a lattice constant of $a = 4.117 \text{ \AA}$.²¹ We believe that the present study of the electronic structure of $\text{Ba}(M_x\text{Sn}_{1-x})\text{O}_3$ with $x = 0.5$ can serve as a qualitative guide for the electronic structure of other member candidates (i.e., $x < 0.5$, as well as possibly for $x < 1$), the calculation of which otherwise will require a very large supercell and ample computational time. We have also theoretically confirmed the feasibility of the formation of stable structures of $\text{Ba}(M_{0.5}\text{Sn}_{0.5})\text{O}_3$ perovskite crystal structure for each system containing tetravalent ion (i.e., $M = \text{Ti}, \text{V}, \text{Cr}, \text{Zr}, \text{Pb},$ and Ce).²² We found that in each of the case the tolerance factor indicated that these $\text{Ba}(M_{0.5}\text{Sn}_{0.5})\text{O}_3$ systems theoretically do form a stable structure.²² Analogous structures have been reported^{23,24} recently, thus supporting the theoretical perception of the present structures studied here.

III. RESULTS AND DISCUSSION

A. Electronic structure of $\text{Ba}(M_{0.5}\text{Sn}_{0.5})\text{O}_3$

Figure 1 displays the total and partial computed densities of states (DOSs) for cubic BSO and $\text{Ba}(M_{0.5}\text{Sn}_{0.5})\text{O}_3$ systems. It clearly demonstrates that there is a trend in the variation of the electronic structure with change of metal ion in $\text{Ba}(M_{0.5}\text{Sn}_{0.5})\text{O}_3$. The common feature is that in all cases the M states, viz., $3d$ (for Ti, V, and Cr), $4d$ (for Zr), $6s$ (for Pb), and $4f$ (for Ce), mainly contribute to the bottom of the conduction band in $\text{Ba}(M_{0.5}\text{Sn}_{0.5})\text{O}_3$, thereby narrowing the band gap as compared to the experimental band gap (3.4 eV) of BSO. In addition, there is also widening of the conduction band width (calculated) for the M ions with reference to that of BSO. Figure 1 indicates that in all cases of $\text{Ba}(M_{0.5}\text{Sn}_{0.5})\text{O}_3$ the low energy DOS between -20 and ~ 8 eV has the main contribution of Ba $6s$, and Sn $4d$ states (along with some low lying states of M). The high energy DOS at the top of valence bands are dominantly constituted of O $2p$. These states also hybridize with Sn $5p$ states to a lesser extent. In the case of the high energy DOS above the Fermi energy (E_F), mainly Sn $5s$ orbitals contribute to the conduction band of BSO. Likewise, for $\text{Ba}(M_{0.5}\text{Sn}_{0.5})\text{O}_3$, (i) respective $3d$ states for $M = \text{Ti}, \text{V},$ and Cr and (ii) Zr $4d$, Pb $6s$, and Ce $4f$ additionally contribute at the bottom of conduction band thereby increasing the conduction band width and effectively reducing the band gap of M systems. Thus

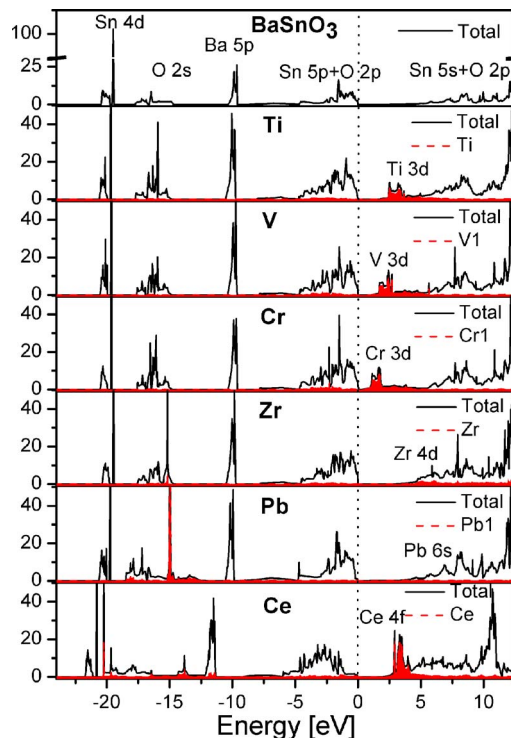


FIG. 1. (Color online) Total and partial DOSs of BSO and $\text{Ba}(M_{0.5}\text{Sn}_{0.5})\text{O}_3$ illustrating the effect of M on DOS. The unit of Y axis is states/(eV/unit cell). The Fermi level is set at 0 eV in each case.

B -site substituted system of ABO_3 with M clearly reveals that there is a dramatic band gap alteration in $\text{Ba}(M_{0.5}\text{Sn}_{0.5})\text{O}_3$. Such kind of doping is known to narrow the band gap of the host lattice. Thus the predicted alteration in band gap of $\text{Ba}(M_{0.5}\text{Sn}_{0.5})\text{O}_3$ is interesting as far as their possible solar energy absorption applications are concerned.

B. Optical properties of $\text{Ba}(M_{0.5}\text{Sn}_{0.5})\text{O}_3$

Figures 2(a) and 2(b) show the results of comparison of the calculated energy dependent absorption coefficient $I(\omega)$ for BSO and doped $\text{Ba}(M_{0.5}\text{Sn}_{0.5})\text{O}_3$ systems in the range of 0–14 eV. The trend in variation shows that Cr has the largest $I(\omega)$ at lower energies than BSO and other doped $\text{Ba}(M_{0.5}\text{Sn}_{0.5})\text{O}_3$ systems, indicating its ability to respond to low energy ($E \leq 2.0$ eV) photons. The $I(\omega)$ curves for the $\text{Ba}(M_{0.5}\text{Sn}_{0.5})\text{O}_3$ systems are significantly different from those of BSO with the main difference that the optical response of $\text{Ba}(M_{0.5}\text{Sn}_{0.5})\text{O}_3$ system is either enhanced and/or red shifted with reference to the optical response of BSO. Especially, $\text{Ba}(M_{0.5}\text{Sn}_{0.5})\text{O}_3$ systems with M as Cr and V systems show higher absorption coefficients than BSO in a low energy range of 0–1 eV. These results of optical property calculation clearly show that $\text{Ba}(M_{0.5}\text{Sn}_{0.5})\text{O}_3$ systems with the M as $\text{Cr} > \text{V} > \text{Ti} > \text{Pb} > \text{Ce} > \text{Zr}$ [in decreasing order of response depending on the $I(\omega)$] respond to the visible or near UV electromagnetic radiation in rather more efficient manner than the cubic barium stannate.

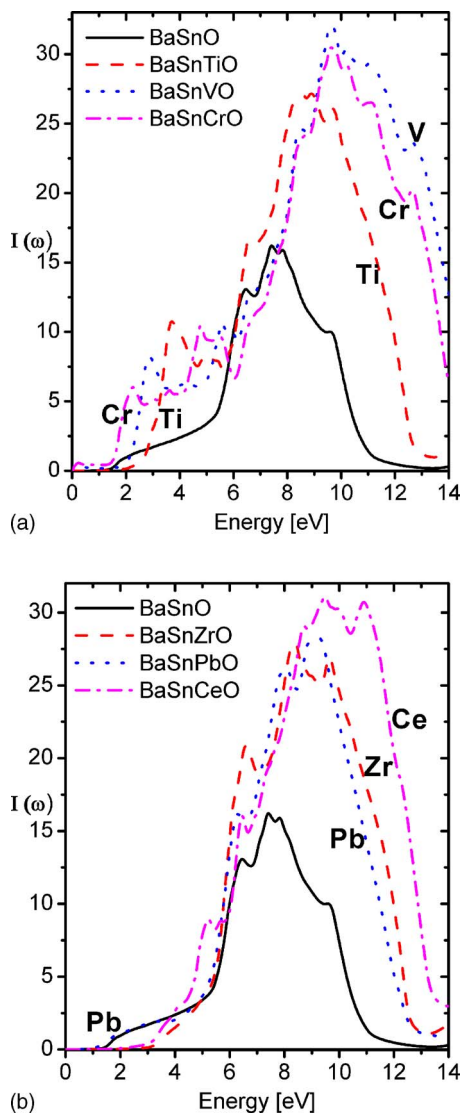


FIG. 2. (Color online) Calculated absorption coefficient $I(\omega)$ of the BaSnO_3 and doped $\text{Ba}(M_{0.5}\text{Sn}_{0.5})\text{O}_3$ structures, as a function of photon energy.

C. Implications on solar and photochemical energy conversion applications

In order to evaluate the physical significance of this work, the results are tabulated and analysis is presented in the form of schematic diagram of Fig. 3. Table I shows the theoretical band gap for each M system. Each individual

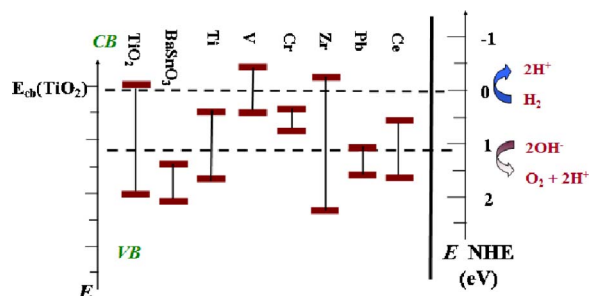


FIG. 3. (Color online) Schematic of valence and conduction band edges estimated from calculated DOS for BaSnO_3 and $\text{Ba}(M_{0.5}\text{Sn}_{0.5})\text{O}_3$ structures, compared with the computed TiO_2 band edge positions (left hand energy axis) and overlaid on NHE scale (Refs. 26 and 27).

TABLE I. The computed band gap for each $\text{Ba}(M_{0.5}\text{Sn}_{0.5})\text{O}_3$ system.

$\text{Ba}(M_{0.5}\text{Sn}_{0.5})\text{O}_3$ for M	Theoretical band gap E_g (eV)
Ti	1.7
V	1.0
Cr	0.3
Zr	2.7
Pb	0.3
Ce	1.6

value reveals that the theoretical band gap is narrowed as compared to the experimental band gap (3.4 eV) of undoped BSO, indicating that the M system can absorb the visible radiation of electromagnetic spectrum. It is noteworthy that the theoretical values have been calculated for $\text{Ba}(M_{0.5}\text{Sn}_{0.5})\text{O}_3$ structure. The calculation implies the possibility of band gap alteration on doping of M ion. However, experimentally one can tailor the band gap as a prerequisite, by the change in $0 < x < 1$ in $\text{Ba}(M_x\text{Sn}_{1-x})\text{O}_3$ system. Thus the work gives a clear qualitative picture of the possible effects of dopant on the DOS with respect to its undoped counterpart.

Our preliminary experimental observation did ensure that doped M -system $\text{Ba}(\text{Pb}_x\text{Sn}_{1-x})\text{O}_3$ absorbed larger wavelengths than those absorbed by BSO. The present theoretical study indicates that the doping can be a guideline to experimentalist to achieve an optically active material for suitable solar applications.

The calculated indirect band gap (0.3 eV) of BSO is found to be underestimated to that of the experimental reported band gap but matches with other theoretical reports.^{8,25} In spite of such underestimation of the calculated band gap, we believe that present type of qualitative study can be worthwhile on relative scale specially for photocatalytic applications. The correctness of the present computational and empirical approach is tested and is evidenced by the case study of TiO_2 , a well known photocatalyst. We used the TiO_2 as a standard candidate and calculated the DOS (not shown). We used its calculated parameters (E_{cb}, E_{vb}) as a reference in further comparative analysis in the later section, within the limits of the calculations and extent of metal doping.

A final analysis of the computed band gap along with their respective optical absorption indicates that the $\text{Ba}(M_{0.5}\text{Sn}_{0.5})\text{O}_3$ systems with $M=\text{Cr}, \text{V}$, and Pb may serve as a better candidate for dry photovoltaic application. However, in the case of photochemical applications, it is not true. This can be analyzed as follows. Figure 3 simplifies the understanding of the above stated fact. Figure 3 presents the comparison of the computed band edge positions of all $\text{Ba}(M_{0.5}\text{Sn}_{0.5})\text{O}_3$ and TiO_2 , a well known photocatalyst, along with the redox levels of water.^{26,27} The E_{vb} (valence band edge) and E_{cb} (conduction band edge) values are obtained from respective DOS curves as received after the calculation of the electronic structures. The detail of the procedure adopted to draw the schematic of Fig. 3 is as follows. We calculated the DOS for anatase TiO_2 (not shown here), from which we obtained the E_{cb} and E_{vb} values and plotted

on an energy scale in eV (left side vertical scale in Fig. 3) as a standard reference. The computed conduction band edge value of TiO_2 is marked as E_{cb} . Thus the obtained energy-level schematic of TiO_2 is overlaid on the normal hydrogen electrode (NHE) scale with respect to the reduction potential (0 eV) and oxidation potential (1.24 eV) of water, depending on the known reports.^{26,27} The diagram shows that the calculated band edge values of TiO_2 lie across the redox levels of water.

Similarly, the E_{cb} and E_{vb} values were obtained from respective DOS spectrum of each $\text{Ba}(M_{0.5}\text{Sn}_{0.5})\text{O}_3$ system and plotted in same way as for TiO_2 , using the left hand energy [E (eV)] axis. Thus the obtained schematic diagram in Fig. 3 was used for further discussions. It has to be noted at this point that in the case of materials in contact with electrolyte, the E_{cb} and E_{vb} values tend to change with changes in the pH, concentration of solvent, and temperature of medium. But one can still rely on the qualitative behavior of the system under consideration. In addition a further uncertainty in the band edges has been schematically displayed by the thick representation of the band edges. Nonetheless, experimentally one can surely tailor-make the electronic structure by proper optimization of concentration of dopants in the $\text{Ba}(M_{0.5}\text{Sn}_{0.5})\text{O}_3$ systems and is in line with our preliminary work on the $\text{Ba}(\text{Pb}_x\text{Sn}_{1-x})\text{O}_3$ system.

The redox levels serve as a guide to compare the $\text{Ba}(M_{0.5}\text{Sn}_{0.5})\text{O}_3$ system with TiO_2 for the suitability of material as visible light photocatalyst or photoelectrochemical applications. TiO_2 , a well known water splitting photocatalyst for years,³ possesses the E_{cb} more negative than the reduction potential of water and E_{vb} more positive than the oxidation potential of water. This is an important condition for water splitting photocatalyst system. Depending on the above stated main criteria of an active water splitting photocatalyst, we discuss and evaluate the $\text{Ba}(M_{0.5}\text{Sn}_{0.5})\text{O}_3$ systems for water splitting photocatalysts. As the E_{cb} and E_{vb} levels $\text{Ba}(M_{0.5}\text{Sn}_{0.5})\text{O}_3$ for $M=\text{Cr}$ lie within the redox levels of water, this condition makes the Cr system unsuitable for the wet photovoltaic applications. The E_{vb} values of BaSnO_3 , $\text{Ba}(M_{0.5}\text{Sn}_{0.5})\text{O}_3$ with M of Ti, Zr, Pb, and Ce, lie more positive than the oxidation potential of water so they are expected to be active only for photo-oxidation. On the contrary, E_{cb} values of $\text{Ba}(M_{0.5}\text{Sn}_{0.5})\text{O}_3$ with M of V and Zr are more negative than the reduction potential of water; thus they are expected to be active for the photoreduction of water. Effectively the theoretical studies indicate that Zr can be an active material for overall photolysis of water under visible light photons.

Furthermore, we investigate the above conclusions taking into consideration the calculated optical property of the systems. Thus though $\text{Ba}(M_{0.5}\text{Sn}_{0.5})\text{O}_3$ for $M=\text{Cr}$ has comparatively larger optical absorption coefficient for $E \leq 2.0$ eV and may make it an active candidate for the dry photovoltaic applications, it is not able to serve as an active candidate for visible light photocatalysis. Depending on the above discussions and the calculated optical absorption coefficients, the remaining M systems can be arranged in the following way in the order of decreasing activity of (i) photo-oxidation by $\text{Pb} > \text{Ti} > \text{Ce} > \text{Zr}$, (ii) photoreduction by

$\text{Zr} > \text{V}$, and (iii) complete photolysis by Zr, in the photoreaction of water under high energy visible light photons ($h\nu \sim 2.5$ eV). It can be further noted that though $\text{Ba}(M_{0.5}\text{Sn}_{0.5})\text{O}_3$ with $M=\text{Zr}$ can possess activity for water splitting under visible light, its poor response towards low energy photons is bound to hamper the efficiency of water splitting. Interestingly our preliminary experimental studies are in accordance with theoretical predictions in the case of $\text{Ba}(\text{Pb}_{0.5}\text{Sn}_{0.5})\text{O}_3$ system. The preliminary results indicates that the Pb system indeed turns into an active visible light photocatalyst (for photo-oxidation of water) in contrast to a completely inactive BSO system. A detailed work is underway.

The theoretical studies, in addition, indicate the suitability of $\text{Ba}(M_{0.5}\text{Sn}_{0.5})\text{O}_3$ with M as (i) Pb, Ti, and Ce systems for photoanode (for photo-oxidation) and (ii) V for photocathode (for photoreduction) in photoelectrochemical applications. It is noteworthy at this juncture that especially Pb has been reported²⁸ recently to be important in inducing visible light activity (mainly for photo-oxidation of water) in perovskites structure. This is in line with the present theoretical study. Thus this study may serve as a very useful guide in solid state material design for wide variety of applications.

IV. CONCLUSION

The paper reports on a comparative study of the theoretically calculated electronic structures and optical properties of cubic BaSnO_3 and cubic $\text{Ba}(M_{0.5}\text{Sn}_{0.5})\text{O}_3$ with $M=\text{Ti}$, V, Cr, Zr, Ce, and Pb, the tetravalent metal ions. The $3d$ orbitals of Ti, V, and Cr, $4d$ of Zr, $4f$ and $6s$ orbitals of Ce and Pb, respectively, contributed to the bottom of the conduction band for narrowing of the band gap of cubic BaSnO_3 . The comparison of computed optical absorption coefficients shows that the $\text{Ba}(M_{0.5}\text{Sn}_{0.5})\text{O}_3$ systems can be arranged for the M under study as (i) $\text{Cr} > \text{V} > \text{Ti}$ and (ii) $\text{Pb} > \text{Ce} > \text{Zr}$, in decreasing order of photoresponse towards low energy photons ($E \leq 2.5$ eV).

ACKNOWLEDGMENT

This work was supported by National Research Laboratory Program, General Motors R&D Center, the Hydrogen Energy R&D Center, the Brain Korea 21 Project, National R&D Project for Nano Science and Technology.

¹K. Ikarashi, J. Sato, H. Kobayashi, N. Saito, H. Nishiyama, and Y. Inoue, *J. Phys. Chem. B* **106**, 9048 (2002).

²J. Sato, H. Kobayashi, K. Ikarashi, N. Saito, H. Nishiyama, and Y. Inoue, *J. Phys. Chem. B* **108**, 4369 (2004).

³A. Fujishima and K. Honda, *Nature (London)* **238**, 37 (1972).

⁴H. Yamashita, H. Harada, J. Misaka, M. Takeuchi, K. Ikeue, and M. Anpo, *J. Photochem. Photobiol., A* **148**, 257 (2002).

⁵K. Kato and A. Kudo, *J. Phys. Chem. B* **106**, 5029 (2002).

⁶M. G. Smith, J. B. Goodenough, A. Manthiram, R. D. Taylor, W. Peng, and C. W. Kimbal, *J. Solid State Chem.* **98**, 181 (1992).

⁷G. Larramona, C. Gutierrez, M. R. Nunes, and F. M. A. daCosta, *J. Chem. Soc., Faraday Trans. 1* **85**, 907 (1989).

⁸H. Mizoguchi, P. M. Woodward, C. H. Park, and D. A. Keszler, *J. Am. Chem. Soc.* **126**, 9796 (2004).

⁹T. R. N. Kutty and R. Vivekanandan, *Mater. Res. Bull.* **22**, 1457 (1987).

¹⁰S. Upadhyay, O. Parkash, and D. Kumar, *Mater. Lett.* **49**, 251 (2001).

¹¹A. Kumar, B. P. Singh, R. N. P. Choudhary, and A. K. Thakur, *J. Alloys Compd.* **394**, 292 (2005).

- ¹²D. W. Hwang, H. G. Kim, J. S. Lee, W. Li, and S. H. Oh, *J. Phys. Chem. B* **109**, 2093 (2005).
- ¹³A. Kudo and H. Kato, *Chem. Phys. Lett.* **331**, 373 (2000).
- ¹⁴M. Miyauchi, M. Takashio, and H. Tobimatsu, *Langmuir* **20**, 232 (2004).
- ¹⁵T. Ishii, H. Kato, and A. Kudo, *J. Photochem. Photobiol., A* **163**, 181 (2004).
- ¹⁶R. Konta, T. Ishii, H. Kato, and A. Kudo, *J. Phys. Chem. B* **108**, 8992 (2004).
- ¹⁷R. Niishiro, H. Kato, and A. Kudo, *Phys. Chem. Chem. Phys.* **7**, 2241 (2005).
- ¹⁸P. Blaha, K. Schwarz, and J. Luitz, WIEN97, improved and updated UNIX version of the original copyrighted WIEN code, Vienna University of Technology, 1997.
- ¹⁹G. Gupta, T. Nautiyal, and S. Auluck, *Phys. Rev. B* **69**, 052101 (2004).
- ²⁰P. H. Borse, H. G. Kim, and J. S. Lee, *J. Appl. Phys.* **98**, 043706 (2005).
- ²¹A. J. Smith and A. J. E. Welch, *Acta Crystallogr.* **13**, 653 (1960).
- ²²M. W. Lufaso and P. M. Woodward, *Acta Crystallogr., Sect. B: Struct. Sci.* **57**, 725 (2001).
- ²³R. N. Das and P. Pramanik, *Nanotechnology* **15**, 279 (2004).
- ²⁴S. W. Ding, J. Wang, Q. Y. Kang, Y. C. Liu, S. J. Liu, and Y. Ding, *Huaxue Xuebao* **60**, 2141 (2002).
- ²⁵R. O. Jones and O. Gunnarsson, *Rev. Mod. Phys.* **61**, 689 (1989).
- ²⁶M. Gratzel, *Nature (London)* **414**, 338 (2001).
- ²⁷T. Bak, J. Nowotny, M. Rekas, and C. C. Sorrell, *Int. J. Hydrogen Energy* **27**, 991 (2002).
- ²⁸H. G. Kim, O. S. Becker, J. S. Jang, S. M. Ji, P. H. Borse, and J. S. Lee, *J. Solid State Chem.* **179**, 1211 (2006).